Molecular Pharmacology 108 (2026) 100137

Molecular Pharmacology

journal homepage: www.molpharm.aspetjournals.org

ARTICLE

Neuroprotective in vitro effects of histone deacetylase 6–selective inhibitor SW-100 toward oxaliplatin-derived toxicity

Angelica Squarzoni [1, 2], Arianna Scuteri [1, *], Elisabetta Donzelli [1], Virginia Rodriguez-Menendez [1], Guido Cavaletti [1]

[1] Experimental Neurology Unit and Milan Centre for Neuroscience, School of Medicine and Surgery, University of Milano-Bicocca, Monza (MB), Italy
[2] PhD Program in Neuroscience, University of Milano-Bicocca, Milan, Italy

ARTICLE INFO

Article history:
Received 31 October 2025
Accepted 3 June 2026
Available online 17 June 2026

Key words:
Neuroprotection
Oxaliplatin
Chemotherapy-induced peripheral neuropathy
Histone deacetylase inhibitors
SW-100

ABSTRACT

Chemotherapy-induced peripheral neuropathy is a common side effect of chemotherapy drugs. Currently, no effective preventive strategies or treatments are available. In recent years, histone deacetylase inhibitors (HDACis), initially approved for hematologic malignancies, have been proposed for neuroprotective purposes. HDACis inhibit histone deacetylases, a group of enzymes involved in the regulation of both histone and nonhistone proteins. In this study, we tested the antitumorigenic abilities of 3 different HDACis (SAHA, romidepsin, and SW-100) in combination with oxaliplatin (OHP) in 3 colorectal cancer cell lines (HT-29, HCT-15, and Caco-2). OHP is the gold standard antineoplastic therapy for the treatment of colorectal cancer, and it is also known to induce peripheral neuropathy, which affects patients' quality of life. OHP treatment often forces a reduction of the clinical effective drug dose, or even an interruption in anticancer treatment. Therefore, we also assessed the efficacy of 3 HDACis in mitigating the neurotoxicity induced by OHP in E15 rat embryo dorsal root ganglia. Apoptotic and cell proliferation pathways were tested through immunoblot analysis, immunofluorescence, and cell survival analysis. The results of this study show that SW-100, a selective histone deacetylase 6 inhibitor, induces apoptosis and reduces cell viability in both HT-29 and HCT-15 when used in combination with OHP. Besides its antineoplastic activity, SW-100 can protect against OHP neurotoxicity, limiting the activation of caspase 3 and selectively inducing α-tubulin acetylation to possibly stabilize axonal transport. In conclusion, we propose SW-100 and OHP as a viable combination for future studies on the treatment of chemotherapy-induced peripheral neuropathy.

Significance Statement: Chemotherapy-induced peripheral neuropathy is a common side effect of oxaliplatin, a drug used for the treatment of colorectal cancer. This study demonstrated that in vitro cotreatment with the histone deacetylase 6 selective inhibitor, SW-100, attenuates the neurotoxic effect of oxaliplatin while maintaining the efficacy of the treatment.

© 2026 The Author(s). Published by Elsevier Inc. on behalf of American Society for Pharmacology and Experimental Therapeutics. This is an open access article under the CC BY license (http://creativecommons.org/licenses/by/4.0/).

1. Introduction

Histone deacetylases (HDACs) are a group of enzymes that catalyze the deacetylation of lysine residues on both histone and nonhistone proteins[1]; they are currently classified into 4 main groups, based on their localization and sequence affinities.[2] HDACs have been extensively studied due to their crucial role in regulating several cellular processes and signaling pathways; although many of their functions remain only partially elucidated, they are now largely recognized for their role in events such as cancer onset and progression, as well as neuronal degeneration.[1] For these

* **Address correspondence to:** Arianna Scuteri, Experimental Neurology Unit and Milan Centre for Neuroscience, School of Medicine and Surgery, University of Milano-Bicocca, Via Cadore 48, Monza (MB), Italy. E-mail: arianna.scuteri@unimib.it

This article has supplemental material available at molpharm.aspetjournals.org.

Current affiliation (A. Squarzoni): Istituto Italiano di Tecnologia (IIT), Genova (GE), Italy.

A. Squarzoni and A. Scuteri contributed equally to this work.

https://doi.org/10.1016/j.molpha.2026.100137
0026-895X/© 2026 The Author(s). Published by Elsevier Inc. on behalf of American Society for Pharmacology and Experimental Therapeutics. This is an open access article under the CC BY license (http://creativecommons.org/licenses/by/4.0/).

reasons, many studies have focused on the effect of their inhibition, with the development of HDAC inhibitors (HDACis) as a class of therapeutics.[2] Currently, HDACis are divided into 2 main classes: selective inhibitors, which are designed to target specific HDACs, and nonselective inhibitors, also known as pan-HDACis. In the early 2000s, the US Food and Drug Administration approved the first HDACi, vorinostat (also known as SAHA), a pan-HDACi, as a treatment for hematologic malignancies.[3]

Following the clinical approval of the first HDACi, these drugs have been tested as potential treatments, either alone or in combination with other therapies, for a wide range of conditions, including cancer and neurodegenerative diseases.[1,4] Among the different HDACs, HDAC6 has recently gained attention because it exhibits a unique molecular structure that distinguishes it from other HDACs, making it an ideal target for the development of specific inhibitors.[5] Moreover, besides cell cycle regulation and mitochondrial transport, it modulates proteins different from histones, such as α-tubulin, and proteins involved in cell survival, such as heat shock protein 90.[6–8] Recent publications suggest that HDAC6 could also be involved in the neurodegenerative cascade pathway.[8] So far, few HDAC6 inhibitors (HDAC6i), like ACY-1215 (ricolinostat) and SW-100, have already been tested for their potential neuroprotective effects, particularly in diseases affecting the central nervous system,[5,7,9–11] but little is known about their anticancer effect.

Besides hematologic diseases, because some studies have suggested a link between elevated levels of specific HDACs and poor prognosis in certain solid tumors, HDACis have also been explored as potential treatments for solid malignancies,[4,12] although with less promising results, probably derived from a lower sensitivity.[9,13,14] One such malignancy tested for HDACi use is colorectal cancer (CRC), which is one of the deadliest cancers worldwide.[15] The current standard treatment for CRC involves the platinum-based drug, oxaliplatin (OHP), which induces DNA cross-linking, disrupting DNA replication and transcription.[16] OHP is typically administered in combination with other chemotherapeutic agents, such as in the FOLFOX regimen.[17] Despite its effectiveness, OHP treatment is often hindered by a limiting side effect represented by the induction of peripheral neuropathy, namely chemotherapy-induced peripheral neuropathy (CIPN).[18]

CIPN is one of the most common and debilitating side effects of chemotherapy, yet there is still no definitive treatment or effective supportive care available.[15] Patients with CIPN experience sensory and motor dysfunctions, either acutely or chronically, depending on the chemotherapeutic drug and treatment regimen.[19] OHP is toxic to the peripheral nervous system, leading to oxaliplatin-induced peripheral neuropathy, which affects sensory neurons and causes symptoms like paresthesia.[20] Despite the high number of patients affected by CIPN, there is currently no approved treatment or preventive measure to alleviate this side effect, which severely impacts patients' quality of life and the socio-economic context in which they live.[15] Consequently, numerous research efforts have been aimed at identifying alternative effective therapies or preventive strategies for CIPN.

Considering the putative antineoplastic and neuroprotective abilities of HDACi, it could be theoretically possible to exploit both by administering them in combination with OHP: on one side, to increase OHP's antineoplastic effect, and on the other side to counteract its neurotoxic action.

This study evaluated whether 3 selected HDACis, namely SAHA, romidepsin (ROMI), and SW-100, used in combination with OHP, could exert antitumorigenic effects in 3 CRC cell lines, and neuroprotective effects in the E15 rat embryo dorsal root ganglia (DRG) model, thus providing new insights into the molecular changes induced by these drug combinations in both experimental systems.

2. Materials and methods

2.1. Cell lines

All the cell lines employed in this research were purchased from American Type Culture Collection (ATCC) and cultured according to the manufacturer's suggestions in a 37 °C humidified incubator with 5% CO_2. Three cell lines were selected to have genetic and phenotypic variability. They are derived from different donors and express different phenotypes and molecular characteristics.

HT-29 cell line (Cat#HTB-38, ATCC) was maintained in RPMI 1640 supplemented with 100 U/mL penicillin, 100 μg/mL streptomycin, and 10% FBS. These cells were initially derived from a female patient; they are currently used as a model for in vitro drug screening, and they have the ability to generate spheroids.[21]

Caco-2 cell line (Cat#HTB-37, ATCC) was maintained in Eagle's minimum essential medium supplemented with 100 U/mL penicillin, 100 μg/mL streptomycin, 10% FBS, and 1 mM sodium pyruvate. This cell line, derived from a male patient, is widely used as an in vitro model for drug screening due to its ability to differentiate.[22]

HCT-15 cell line (Cat#CCL-225, ATCC) was maintained in RPMI 1640 supplemented with 100 U/mL penicillin, 100 μg/mL streptomycin, 10% FBS, 10 mM HEPES, and 1 mM sodium pyruvate. This cell line is a model widely used for in vitro drug screening, which is derived from a male patient affected by CRC.[23,24]

All the cell culture media and supplements used were purchased from Euroclone S.p.A.

2.2. Drugs

OHP (Selleckchem Chemicals) was dissolved at 3 mM in bidistilled water and stored at −20 °C. SAHA (Merck KGaA), ROMI (Merck KGaA), and SW-100 (MedChemExpress) were solubilized at 20 mM, 1 mM, and 20 mM, respectively, in DMSO, stored as aliquots at −80 °C, and utilized within a 2-month period.

2.3. Cell survival assay

Cell survival of HT-29, Caco-2, and HCT-15 cell lines treated with SAHA, ROMI, SW-100, and OHP was evaluated by means of sulphorodamine-B (SRB) assay. All the chemicals used for the SRB assay were purchased from Merck KGaA.

The CRC cell lines were plated 5000 cells/well in 96 multiwell plates (Euroclone S.p.A.) in the appropriate cell culture medium and incubated for 24 hours (Caco-2 cell line) or 48 hours (HT-29 and HCT-15 cell lines) before treatment. The drugs were diluted in complete medium and added to the wells to obtain the concentrations detailed in Table 1. For each drug, we chose an initial range of concentration according to the literature and manufacturers' reports. Control untreated cells were set for each cell line. For each cell line, at least 2 experimental sessions were performed with 3 replicates for each concentration.

Cells were returned to the incubator and, after 48 hours, were fixed by adding 10% trichloroacetic acid 20 μL/well and incubating at 4 °C for 1 hour. The 96 multiwell plates were then washed with running water 4 times and dried. The plates were stained by adding 50 μL of 0.4% SRB in 1% acetic acid to each well, incubated for 15 minutes, washed 4 times with 1% acetic acid, and subsequently completely dried. The SRB staining was then solubilized by adding 10% tris(hydroxymethyl)aminomethane 100 μL/well.

Table 1
Drug concentrations assessed by the SRB cell viability assay to determine the IC_{50} in the 3 cell lines

Cell Line	OHP	SAHA	ROMI	SW-100
	μM	*μM*	*nM*	*μM*
HT-29	0.015, 0.5, 1, 2, 2.5, 4, 5, 25, 50	0.2, 0.5, 0.75, 1, 1.25, 1.5, 2, 2.5, 5, 10	1.4, 1.5, 5, 10, 20	0.015, 0.5, 8, 9.5, 10, 20, 25, 50
Caco-2	0.015, 0.5, 1, 2.5, 5, 7.5	0.2, 0.5, 0.75, 1, 2, 5, 10, 15, 20	1, 5, 7.5, 9, 20, 50	1, 2.5, 3.5, 7.5, 10, 25, 50
HCT-15	0.015, 0.5, 1, 2.5, 5, 10	0.2, 1, 2, 5, 10, 15	100, 200, 300, 500, 600, 800	0.5, 1, 2.5, 5, 7.5, 10, 25

Optical density was read at 510 nm with FLUOStar Omega (BMG LABTECH), and the resulting values were used to calculate cell survival by subtracting the value of absorbance obtained by the media alone and comparing each sample with the corresponding untreated control representing the 100% reference. The IC_{50} values were obtained with the software Origin 2023b (OriginLab Corporation). The IC_{50} was generated by obtaining one curve pooled from the experiments. We used the nonlinear curve fit (DoseResp) embedded in Origin software, imposing top = 100%, bottom = 0%, and slope free to vary, with exceptions for Caco-2 + OHP and Caco-2 + SAHA. These per-curve fitting choices were made based on inspection of the data (further details in Supplemental Table 1).

The parameters of each cell line and treatment were chosen based on the fitting curve generated with the dose-response model. The parameters varied based on the curve.

The combination treatments were performed by using the IC_{50} concentration of each different drug, combining each HDACi with OHP. The SRB assay was performed as described above after a 48-hour treatment of HT-29, HCT-15, and Caco-2. The seeding method, assay, absorbance quantification, and data analysis were the same as described above.

2.4. DRG explants

DRG primary neuronal cultures were established according to previously published protocols.[25] Briefly, DRGs were microsurgically dissected by E15 rat embryos derived from a Sprague-Dawley pregnant rat (Envigo). All experiments have been performed in accordance with the Institutional Animal Care and Use Committee for the institution and follow national guidelines and regulations.

For DRG organotypic cultures, the isolated intact DRGs were plated 4/dish on 35 mm collagen-coated dishes in AN2 medium, composed of minimum essential medium supplemented with 0.6% glucose (Merck KGaA), 50 μg/mL L-ascorbic acid (Merck KGaA), 1.4 mM L-glutamine, 10% calf bovine serum (CBS), and 5 ng/mL NGF. After 2 hours, DRGs were treated with different drugs for 24 and 48 hours. For each treatment, we set up 4 different dishes, each containing at least 4 DRGs. At the end of the treatment, pictures of DRG organotypic cultures were captured with Nikon Optical Microscope and Leica DFC290 HD, and for each dish, the longest neurite was measured with Fiji ImageJ (National Institutes of Health). Each experiment was performed 3 times. In this way, for each experiment, we measured 16 neurites/sample, repeated 3 times. At the end, a one-way ANOVA on the per-experiment means has been performed.

For the establishment of DRG primary neuronal cultures, DRGs were collected in Leibovitz's L-15 medium, and a mechanical and enzymatic dissociation was performed. The resulting cellular suspension was seeded 1 drop/dish on 35 mm collagen-coated gridded dishes (corresponding to 25−50 DRGs/dish) in the same AN2 medium used for organotypic culture but containing 15% CBS and supplemented with 10^{-5} M 5-fluoro-2′-deoxyuridine for 5 days. Afterward, the medium was replaced with AN2 containing 15% CBS without 5-fluoro-2′-deoxyuridine.

In both organotypic DRGs and neuronal cultures, treatments with drugs (alone and in combination with OHP) at the IC_{50} values calculated for the HT-29 cell line were performed for 48 hours.

Neuronal cultures were lysed to obtain protein extracts for western blotting analysis.

2.5. Immunoblotting analysis

Cell lysates were obtained after 48 hours of treatment from HT-29, HCT-15, and Caco-2 cells and from DRG neuronal cultures as previously described[25] and quantified with the Bradford technique. Ten μg/well of proteins were run onto 13% SDS-PAGE with prestained protein SHARPMASS VII Marker (Euroclone S.p.A.) as a protein ladder. Afterward, proteins were transferred to a nitrocellulose membrane (Amersham Protran 8, Cytiva, Merk Life Science S.r.l.).

Both primary and secondary antibodies were diluted in the blocking buffer according to the manufacturer's instructions (see Table 2 for dilutions and manufacturers' details). Membranes were incubated with primary antibody overnight at 4 °C, rinsed in the washing buffer, and subsequently incubated with the secondary antibody for 1 hour at room temperature.

Immunoreactive proteins were visualized using a chemiluminescence system (Euroclone S.p.a.), and images were acquired with Amersham Imager 600 (GE Healthcare).

2.6. Immunofluorescence analysis

The cells and primary neuronal cultures were seeded on glass coverslips as previously described and treated for 48 hours. Cells were fixed in 4% paraformaldehyde, washed with PBS, and incubated in 0.1 M glycine for 5 minutes. After being rinsed in PBS, coverslips were incubated in a blocking buffer (5% bovine serum

Table 2
Primary antibodies used for western blot and immunofluorescence analysis

Antibody	Manufacturer	Dilution
Monoclonal anti-tubulin, acetylated antibody, cat#T6793	MilliporeSigma (Merck KGaA)	1:1000
Anti-β-actin (ACTB) antibody, cat#A1978	MilliporeSigma (Merck KGaA)	1:1000
Monoclonal anti-tubulin, acetylated antibody, cat#T6793	MilliporeSigma (Merck KGaA)	1:100
Cleaved caspase-3 (Asp175) antibody, cat#9661	Cell Signaling Technology	1:100
Cleaved caspase-7 (Asp198) (D6H1) rabbit mAb, cat#8438	Cell Signaling Technology	1:100
Anti-NeuN antibody, clone A60, cat#MAB377	MilliporeSigma (Merck KGaA)	1:100

albumin and 0.5% Triton) for 1 hour. Afterward, coverslips were incubated overnight at 4 °C with the primary antibodies diluted in blocking buffer. The list of the primary antibodies used, and the working dilutions, is reported in Table 2.

The day after, coverslips were rinsed in PBS and subsequently incubated for 1 hour at room temperature with the appropriate secondary antibodies diluted 1:200 in PBS. Alexa Fluor 555 Phalloidin (Cell Signaling Technology, cat#8953) was added to the secondary antibody 1:200 to stain actin and incubated. Subsequently, coverslips were rinsed in PBS and mounted using a mounting solution supplemented with 4′,6-diamidino-2-phenylindole (DAPI) (Merck KGaA) to stain nuclei. The images were then captured with a Zeiss LSM 710 Confocal Microscope (ZEISS).

2.7. Statistical analysis

The calculation of the IC_{50} of each drug in the 3 CRC cell lines was performed with the OriginPRO 2023b software (OriginLab Corporation).

The combination treatment results were expressed as mean percentage ± SD and were analyzed with one-way ANOVA test, and Tukey post-test analysis with GraphPad Prism (version 8; GraphPad Corp).

Immunoblotting images were analyzed with the Fiji ImageJ (National Institutes of Health) quantification tools to obtain densitometric data. Because densitometry ratios could be considered closer to lognormal than normal,[26] immunoblotting analysis results were analyzed with a one-way ANOVA test, Tukey post-test analysis with GraphPad Prism, and presented as geometric means with 95% CIs on the log scale.

The graphs were generated with GraphPad Prism. The images, graphs, and pictures were arranged into figures with Adobe Photoshop 2025 (Adobe Inc).

3. Results

3.1. Effects of HDACis in CRC cell lines

3.1.1. Determination of the IC_{50} values

The first step was the evaluation of the cytotoxic effect of the selected HDACs (SAHA, SW-100, ROMI) in 3 different CRC cell lines, namely HT-29, Caco-2, and HCT-15. Cytotoxicity was determined by calculating the IC_{50} for each drug and cell line by using the SRB assay after 48 hours of drug exposure. The same analysis was also performed for OHP.

IC_{50} values calculated for each drug vary across the 3 CRC cell lines and were used to select the drug concentrations for further combination experiments (Table 3). Supplemental Table 1 provides further details on IC_{50} calculation.

3.1.2. Combination treatments

The IC_{50} values previously determined were then used in combination with OHP to ascertain the putative potentiation of anticancer effect. Combination treatments were performed to evaluate cancer cell viability after 48 hours of cotreatment, and the results obtained were compared to treatment with OHP alone (detailed statistical analysis is reported in Supplemental Table 2). This step was crucial in determining whether the combination treatments performed better than OHP alone in reducing cancer cell viability.

In the HT-29 cell line, each HDAC in combination with OHP resulted in a modest but statistically significant increase in cell death compared to OHP alone in a statistically significant manner, as shown in Fig. 1A. The SAHA + OHP treatment resulted in a decrease of around 12% cell survival compared to OHP. The SW-100 + OHP treatment reduced cell viability by 20% with respect to OHP. In the case of ROMI + OHP, cell viability decreased by around 26% compared to treatment with OHP, and it was very similar to ROMI alone.

Similar results were observed in the HCT-15 cell line (Fig. 1B), with a statistically significant reduction in cell survival in the combination treatments, SAHA + OHP and SW-100 + OHP, compared to OHP alone. The combination, SAHA + OHP, decreased the cell viability by 16% compared to OHP alone, whereas it decreased by around 14% and 13% in SW-100 + OHP and ROMI + OHP, respectively, compared to OHP alone. The combination, ROMI + OHP, resulted in a nonstatistically significant reduction of cell viability compared to OHP.

In the case of the Caco-2 cell line (Fig. 1C), none of the combination treatments showed a statistically significant difference in cell death with respect to OHP alone. The SAHA + OHP, ROMI + OHP, and SW-100 + OHP decreased cell viability by around 5%, 2%, and 4%, respectively, compared to OHP alone.

3.1.3. Caspase 3 and caspase 7 activation in the HT-29 cell line

Because the HT-29 cell line is the most sensitive to all combination treatments, we focused on these cells to characterize the cell death by analyzing the activation of different caspases, key proteins involved in apoptosis. Concerning the drugs, we narrowed down our attention to SAHA and SW-100, the 2 compounds able to increase OHP anticancer activity in 2 of the 3 cancer cell lines analyzed. Moreover, the 2 drugs are a pan-HDACi and a selective HDAC6i, respectively; thus, the comparison could shed light on the possibility of acting on specific members of the HDAC family to modulate biological pathways.

Starting from the literature reports demonstrating the apoptosis induction by OHP in cancer cells,[16,24] to characterize the cell death in our model, we evaluated the presence of the cleaved active form of caspase 3 and caspase 7 in cells treated with OHP, SW-100, and SAHA, and their combination.[27] HT-29 cells were treated for 48 hours with OHP, SAHA, SW-100, SAHA + OHP, or SW-100 + OHP, and a qualitative analysis of caspase active forms was then performed by immunofluorescence staining (Fig. 2).

As shown in representative pictures in Fig. 2A, all the samples analyzed exhibited the presence of cleaved caspase 3, even if with a different intracellular distribution. In controls, a predominantly punctate cytoplasmic signal was observed, with only a few positive nuclei. On the contrary, in OHP-treated cells, the signal was clearly nuclear. SAHA-treated cells displayed a nuclear staining with an uneven appearance coupled to a diffuse signal in the cytoplasm, even if less evident than in controls. In cells treated with SAHA + OHP, this diffuse cytoplasmic signal was more evident, and a few positive nuclei were also present, resulting in a pattern similar to that observed in control cells. The treatment with SW-100 resulted in a peculiar distribution of the immunostaining, with a diffuse, low, and mainly cytoplasmatic signal coupled to some spots in the cytoplasm. A few positive nuclei were also evident. The cotreatment of SW-100 and OHP resulted in a

Table 3
Drug concentrations used in combination experiments
Drug concentrations (based on IC_{50} calculation) used in combination experiments for the 3 colorectal cancer cell lines (HT-29, Caco-2, and HCT-15). Details for the IC_{50} calculation are provided in Supplemental Table 1.

Cell Line	OHP	SAHA	ROMI	SW-100
	μM	μM	nM	μM
HT-29	4.8	0.9	2.5	15
Caco-2	2.5	2	5.7	7.7
HCT-15	2.3	6.2	370	8.2

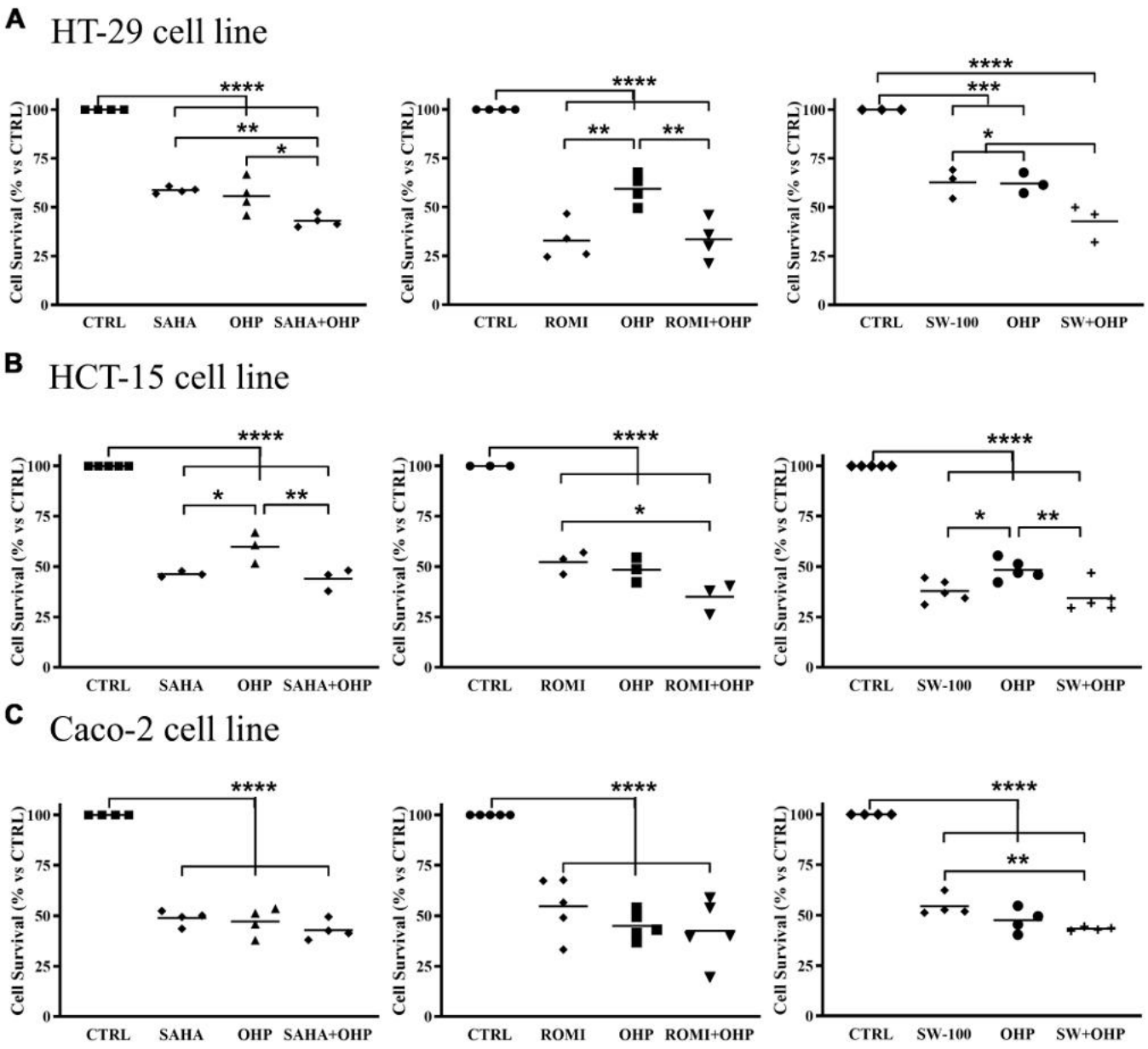

Fig. 1. Cell survival evaluation in cancer cells. Cell survival percentage after 48 hours of treatment with SAHA, romidepsin, and SW-100 in combination with OHP, compared to OHP alone and to the different HDACis, for HT-29 colorectal cancer cell line (A), HCT-15 colorectal cancer cell line (B), and Caco-2 colorectal cancer cell line (C). The drug concentrations used in each cell line are specified in Table 3. For each cell line, 3 experimental sessions were performed, with 3 replicates for each session. The obtained data were analyzed with a one-way ANOVA test and Tukey post-test analysis with GraphPad Prism. Scatter plots with mean values were reported in graphs. *$P < .05$; **$P < .001$; ***$P < .001$; ****$P < .0001$.

nuclear staining not different from that observed in cells treated with OHP alone, suggesting that SW-100 did not interfere with the OHP-induced apoptosis in HT-29 cells.

Also, cleaved caspase 7 was present in all the analyzed samples with different features (Fig. 2B). In control cells, we observed homogeneous staining, spread in the cytoplasm as well as in the nuclei with small dots. Cells treated with OHP displayed a mainly nuclear signal, with a very low cytoplasmic component. SAHA treatment resulted in homogeneous cytoplasmic and nuclear staining without the dots observed in the control. A few nuclei were also positive. The cells treated with SAHA + OHP displayed a mainly nuclear signal, similar to the pattern observed in OHP-treated cells. The treatment with SW-100 resulted again in homogeneous cytoplasmic and nuclear staining, stronger in close proximity to the nuclei. Cotreatment with SW-100 and OHP resulted in a dotted and homogeneous cytoplasmic and nuclear staining, similar to the control cells.

3.2. Evaluation of the neuroprotective effect of HDACis against OHP neurotoxicity in DRGs

We further moved to ascertain the putative neuroprotective effect of HDACs by evaluating neurite elongation in E15 rat embryo–derived DRG, a reliable method to assess neurotoxicity.[25] Based on the promising results observed in the HT-29 cell line, we treated DRGs for 48 hours with SAHA, ROMI, SW-100, OHP, and their combination at the IC_{50} values previously identified in HT-29 cells.

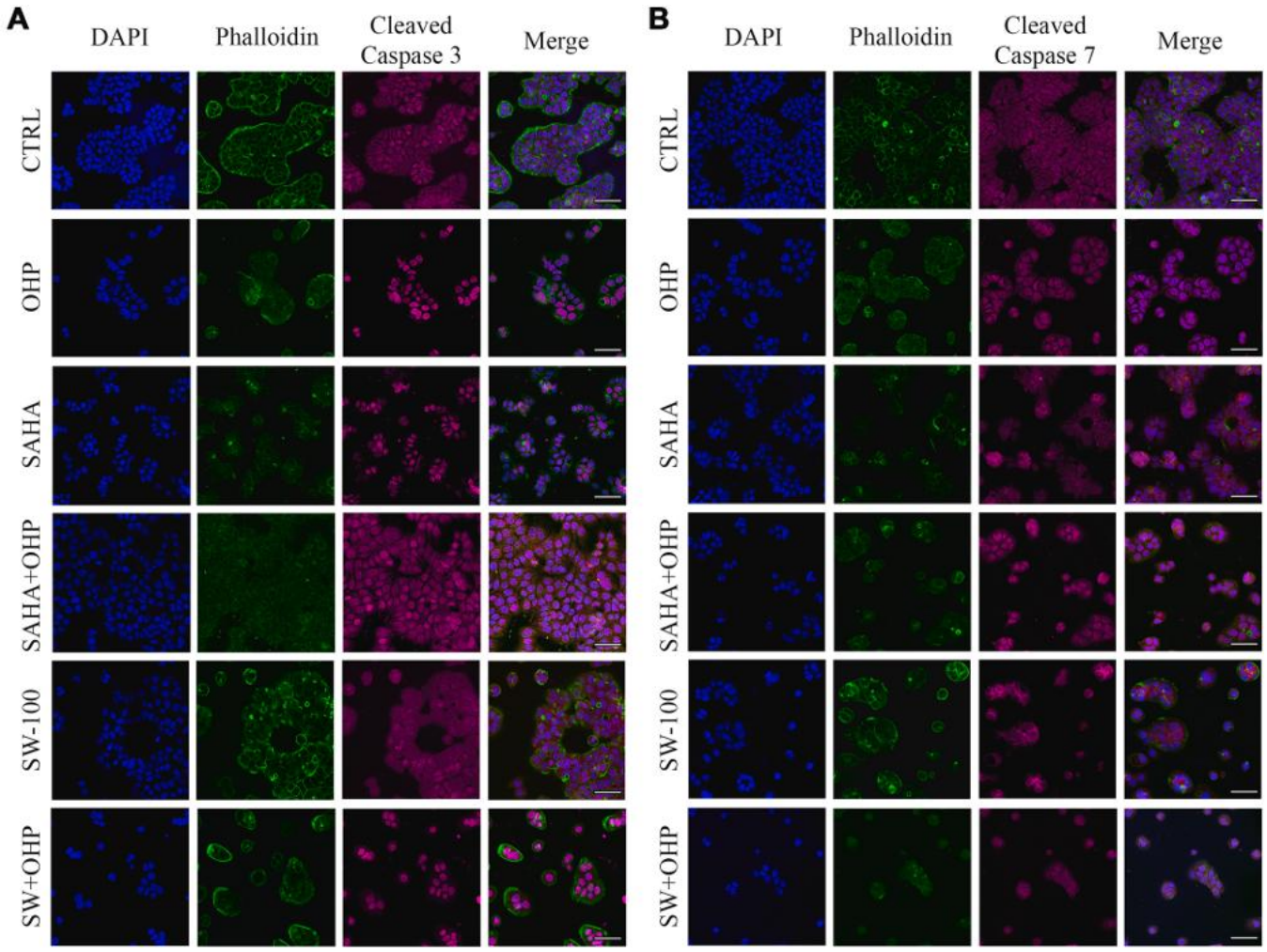

Fig. 2. Cleaved caspases detection in cancer cells. Immunofluorescence analysis for cleaved caspase 3 (A) and cleaved caspase 7 (B) in the HT-29 cell line treated for 48 hours with OHP, SAHA, SAHA + OHP, SW-100, and SW-100 + OHP. 4′,6-diamidino-2-phenylindole (DAPI) staining in blue, phalloidin staining in green, and cleaved caspases staining in red. Scale bar, 50 μm.

We observed that OHP reduced the neurite outgrowth of DRG after 24 hours (data not shown) and 48 hours of treatment by more than 50% with respect to control untreated DRGs. On the contrary, both SW-100 and ROMI did not induce any neurotoxic effect, with a neurite length similar to the control one, whereas DRGs treated with SAHA alone showed a neurite length about 25% shorter than the control, although higher than OHP-treated DRGs (Fig. 3A).

Concerning the cotreatments, the SAHA + OHP combination failed to protect against OHP neurotoxicity (Fig. 3B), resulting in a neurite length reduced in both compared to OHP alone and to SAHA alone. On the contrary, ROMI exerted a neuroprotective effect toward OHP neurotoxicity (Fig. 3C), with the combination ROMI + OHP resulting in a reduced neurite length compared to control untreated DRGs but increased compared to treatment with OHP alone. A similar and even more interesting result was observed in DRGs treated with SW-100 + OHP (Fig. 3D), which exhibited the greatest neurite length among the combination-treated groups, thus suggesting that this HDAC6i significantly protected against OHP-induced neurotoxicity.

3.3. Analysis of caspase 3 activation in DRG-derived neurons

We further moved to evaluate the cellular death occurring in DRG neuron primary cultures after exposure to different HDACs, alone or in combination with OHP. We focused our attention on SW-100, being the most neuroprotective compound, and on SAHA, which was, on the contrary, ineffective toward OHP neurotoxicity. Immunofluorescence analysis of cleaved caspase 3 was performed, therefore, on neurons treated with OHP, SAHA, SW-100, and their combinations.

Although not a quantitative evaluation, immunofluorescence analysis qualitatively corroborated the neurotoxicity assessment. In fact, as shown in representative pictures in Fig. 4, the active cleaved form of caspase 3 was nearly absent in the major part of control neurons, even if a few of them were positive for cleaved caspase 3 and showed morphological features of cellular degeneration. On the contrary, cleaved caspase 3 was observed in most of the OHP, SAHA, SAHA + OHP, and SW-100–treated neurons; SW-100 + OHP resulted in a few neurons strongly positive in the nuclei, similarly to control untreated neurons.

3.4. Analysis of molecular mechanisms potentially involved in neuroprotection

The acetylated form of α-tubulin has been reported to promote axonal integrity and transport.[28,29] Because HDACs, and in particular HDAC6,[8,11,14] could affect α-tubulin acetylation, we investigated

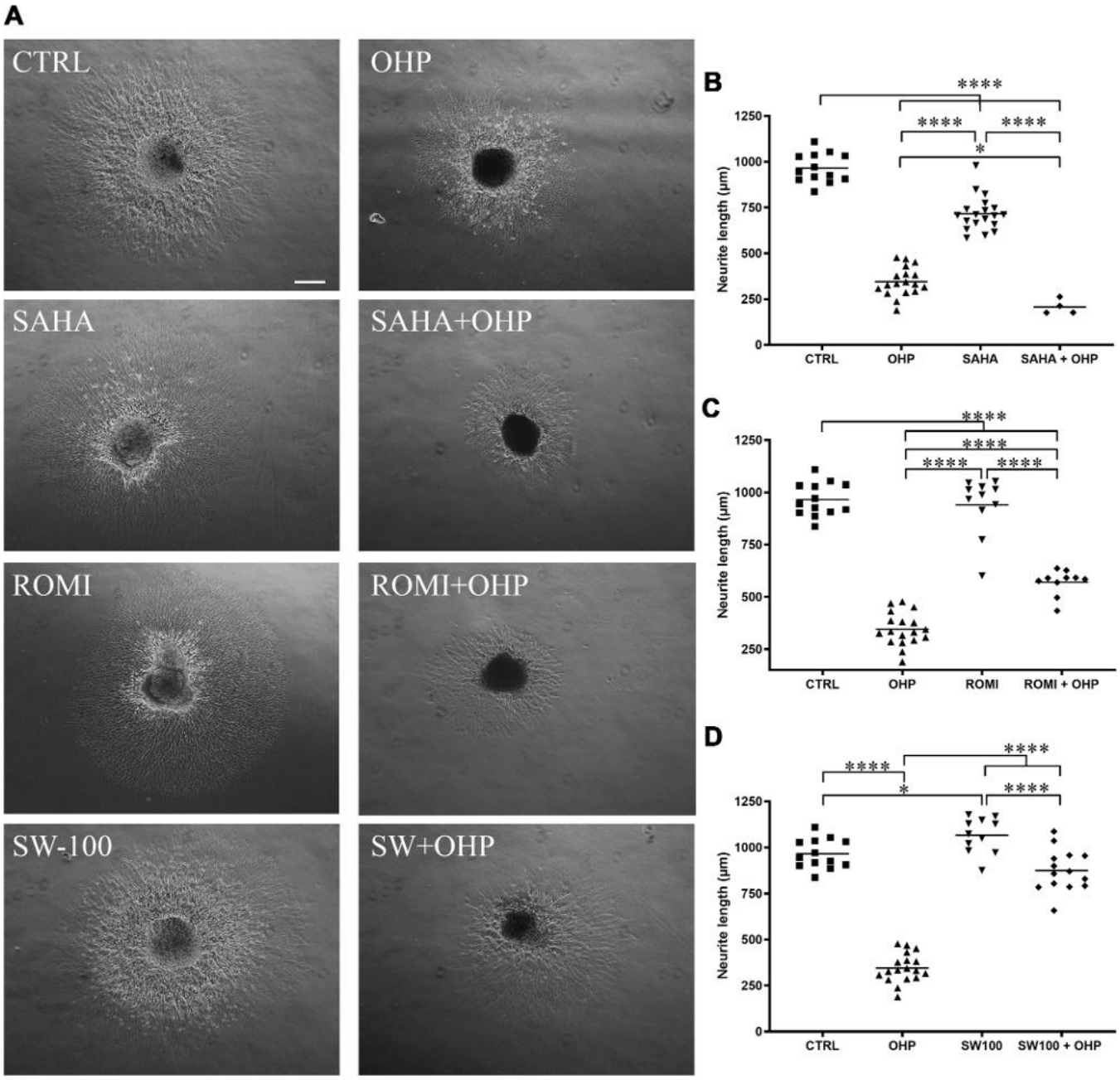

Fig. 3. Evaluation of neurite elongation in DRGs treated for 48 hours with OHP, HDACis, and their combinations. Representative pictures are shown in (A) (scale bar, 300 μm). The longest neurite in each sample was measured. The experiments were performed 3 times. Neurite length as scatter plots with mean values were reported in graphs (B–D). *$P < .05$; ****$P < .0001$.

the effect of both SAHA (pan-HDACi) and SW-100 (HDAC6-specific inhibitor) on this protein in DRG-derived neurons.

The western blot analysis evidenced a basal level of acetylated α-tubulin in untreated neurons that was not modified in neurons exposed to OHP alone. After exposure to SAHA, both alone and in combination with OHP, acetylated α-tubulin resulted in increased levels, and a similar and even more evident increase was observed in neurons treated with SW-100, both alone and with OHP (Fig. 5, A–C and Supplemental Fig. 1). This result was not unexpected, considering the biological activity of these drugs; however, the great variability among the experiments did not allow for obtaining statistically significant results.

To better outline the putative role of acetylated α-tubulin, we analyzed its distribution in neuronal processes by immunofluorescence. As shown in Fig. 5D, control neurons display intact neurites. On the contrary, OHP treatment resulted in a fragmented appearance of the neurites, evidenced by acetylated α-tubulin immunostaining. The same feature, but at a reduced degree, was observed in SAHA-treated neurons, and even more after the exposure to OHP in combination with SAHA. No signs of neurite fragmentation were observed in neurons treated with SW-100 alone nor in combination with OHP, suggesting that the cotreatment of SW-100 and OHP was able to preserve neurite integrity.

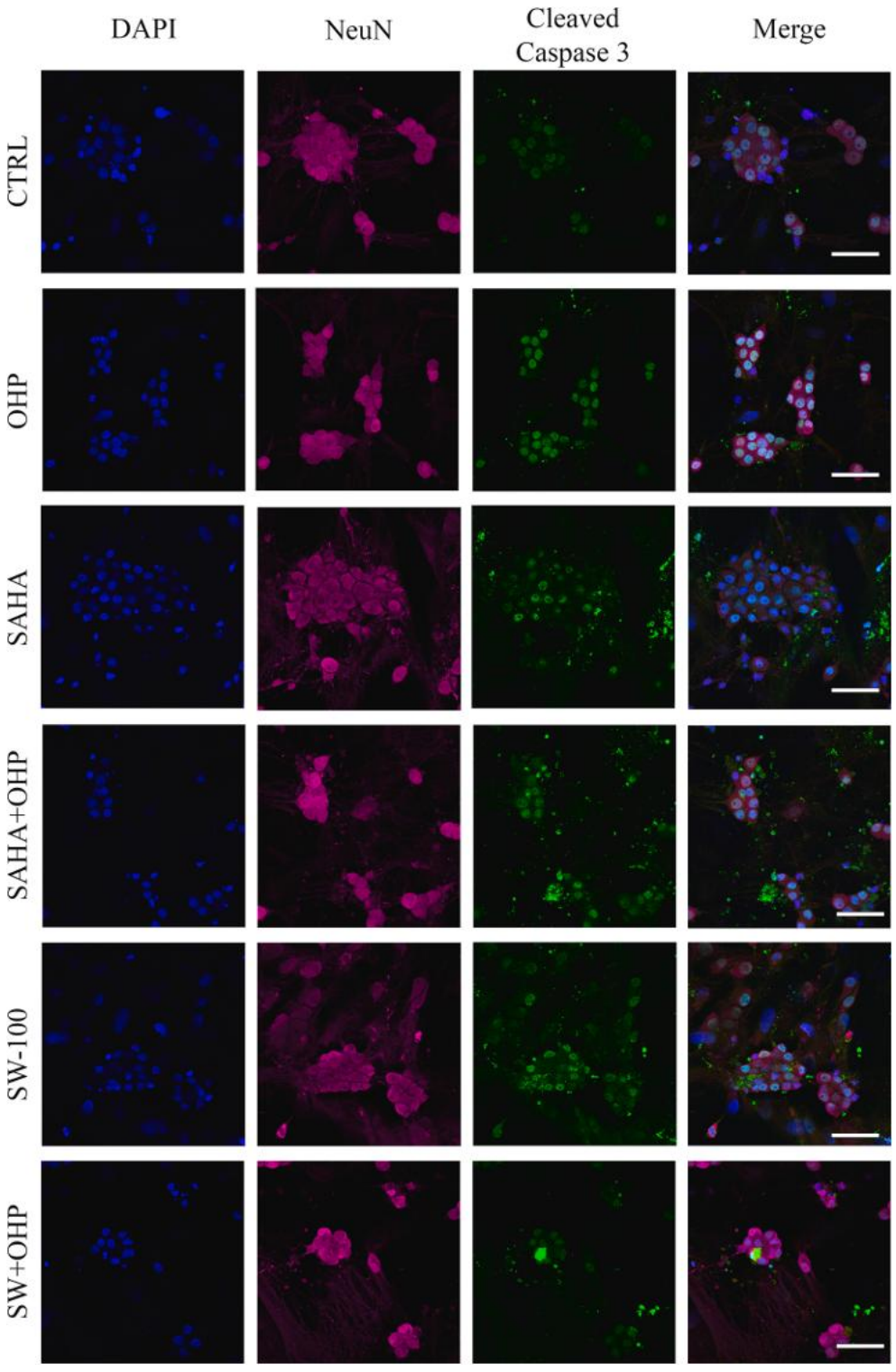

Fig. 4. Cleaved caspases detection in DRG neurons. Immunofluorescence analysis for cleaved caspase 3 in DRG neurons after 48 hours of treatment with OHP, SAHA, SAHA + OHP, SW-100, and SW-100 + OHP. In blue 4′,6-diamidino-2-phenylindole (DAPI) staining, in magenta NeuN, and in green cleaved caspase 3. Scale bar, 20 μm.

4. Discussion

OHP-induced neurotoxicity is a fundamental challenge in cancer treatment, leading to extensive research aimed at mitigating its side effects while maintaining the drug's efficacy against CRC.[20,30] Despite efforts, clinical strategies for preventing CIPN have been largely unsuccessful.[15,31,32] As a result, there has been an increased focus on epigenetic modifiers, such as HDACis, as a tool to potentially reverse or reduce neurotoxic effects without compromising the drug's antitumor efficacy.[1]

In various clinical settings, HDACis have attracted attention due to their ability to modulate a broad spectrum of cellular

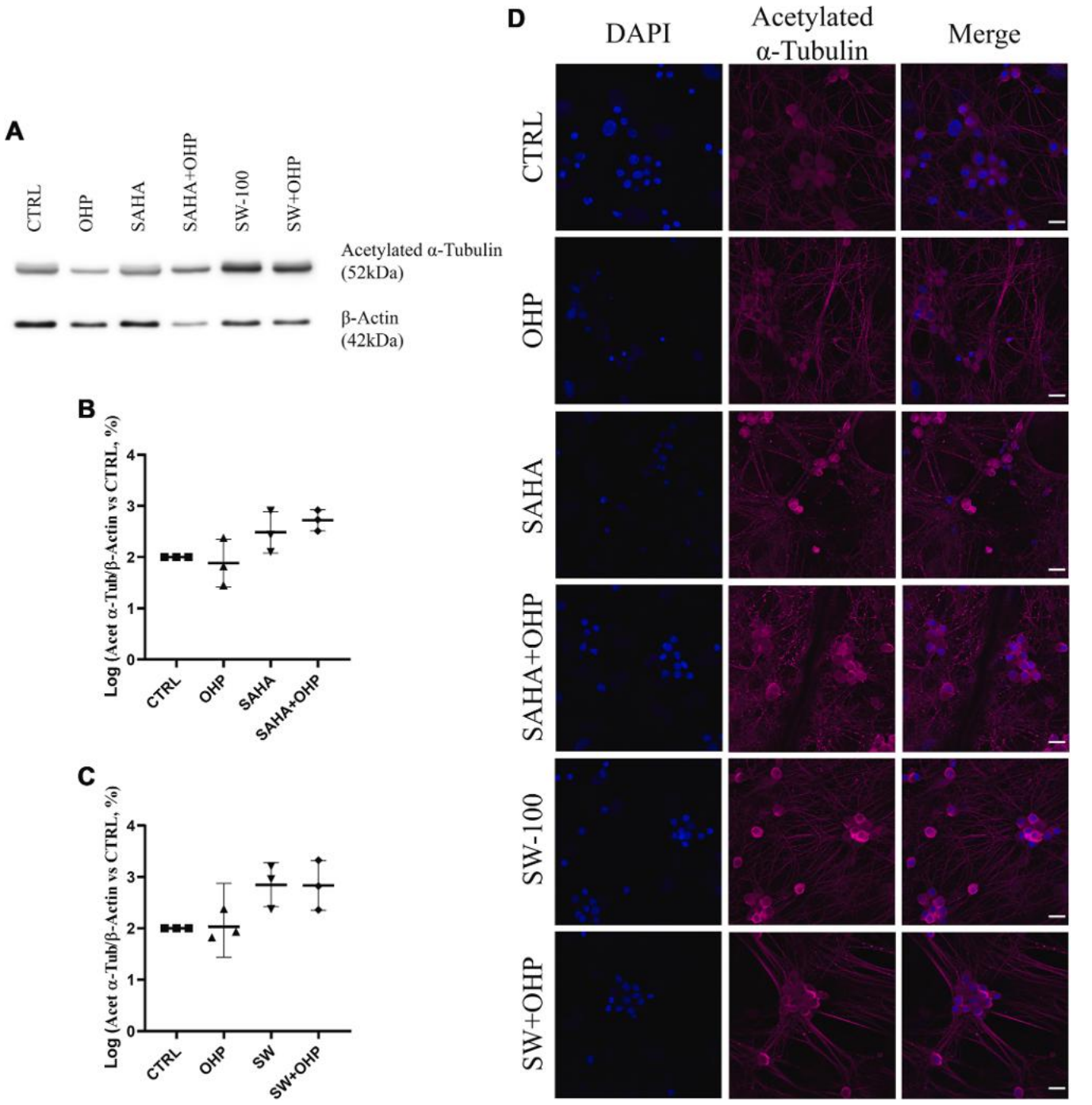

Fig. 5. Analysis of acetylated α-tubulin in DRG neurons. Representative western blot (A) and densitometric analysis (averaged from 3 independent experiments) obtained from the DRG neurons treated for 48 hours with OHP, SAHA, SAHA + OHP (B), or OHP, SW-100, SW-100 + OHP (C). β-Actin represented the loading control and was used as a reference for densitometric analysis, which is reported in scatter plots with geometric mean values with 95% CI on a log scale of the percentage of acetylated α-tubulin/β-actin with respect to control. (D) Immunofluorescence analysis of the DRG neurons treated with OHP, SAHA, SAHA + OHP, SW-100, and SW-100 + OHP for 48 hours and stained with antiacetylated α-tubulin antibody (in magenta) and 4′,6-diamidino-2-phenylindole (DAPI) (in blue) to visualize the nuclei. Scale bar, 20 μm. Each experiment was repeated 3 times. The original western blots are provided as Supplemental Fig. 1.

pathways.[1,10,30] HDACis have been explored for their potential in different models of neurodegeneration.[1] Intriguingly, previous studies have suggested that HDAC6 inhibitors can alleviate symptoms of neurotoxicity in preclinical models of cisplatin-induced and paclitaxel-induced peripheral neuropathy, pointing to a possible therapeutic avenue for protecting against chemotherapy-induced nerve damage.[33–35]

In this study, we aimed to identify an HDACi that could reduce OHP-induced neurotoxicity while enhancing (or at least preserving) its antitumor activity in CRC models.

Our results indicated that SAHA and SW-100, in combination with OHP, exhibited the most relevant cytotoxic effects in HT-29 and HCT-15 cell lines. The HT-29 cell line, most of all, was sensitive to all 3 HDACis when used in combination with OHP, making it

the most promising model and, for this reason, selected for further molecular characterization. In contrast, the Caco-2 cell line showed no statistically significant differences in viability with combination treatments, highlighting the variability of drug responses in different CRC models. Histone acetylation is variable in humans, potentially explaining why the 3 different CRC cell lines considered in this study have different sensitivities to HDACis.[36]

Next, we investigated the molecular mechanisms underlying the observed cytotoxicity. CRC cells often evade apoptosis, a key cell death pathway, which is one of the main reasons for treatment resistance.[37] The cell death characterization confirmed the occurrence of apoptotic death after the exposure of HT-29 cells to OHP; the molecular analysis revealed that HDACis also shared the effect of OHP gold standard therapy on cell death induction, both alone and in combination with it. Intriguingly, our results demonstrate that the combination of SAHA and OHP-induced apoptotic cell death through caspase 7 activation, while SW-100 in combination with OHP exerted the same action by caspase 3 activation. This observation emphasizes once again that even if both the drugs are HDACis, their different specificity may reflect in the activation of different molecular pathways.

The increase in cell death observed after the exposure of HT-29 to the combination of OHP and HDACis, although statistically significant, was probably too limited to be considered biologically important, and it could be potentially ascribable to an additivity effect.

Of greater relevance were the findings regarding the neuroprotective potential of HDACis. OHP is well known to induce apoptosis and neurotoxicity in the peripheral nervous system.[20,38] In our study, SW-100 and OHP combination treatment showed the most relevant protective effect on neurite elongation. In contrast, when SAHA was combined with OHP, it failed to prevent neurite damage.

The induction of apoptosis in DRG-derived neurons was demonstrated by the presence of active, cleaved caspase 3, particularly in the OHP-treated neurons.[27] However, SW-100 was able to reduce apoptosis in the presence of OHP, further supporting its stronger neuroprotective potential. These findings suggest that SW-100, a specific HDAC6 inhibitor, has the unique ability to protect against OHP-induced neurotoxicity while promoting neuronal survival. In particular, according to our data, the downregulation of HDAC6 allowed neurite outgrowth levels comparable to untreated DRG, while increasing α-tubulin acetylation in DRG. This result is consistent with prior literature, where cleaved caspases were observed in peripheral neuropathy in small fibers in a rat model after treatment with vincristine.[39]

We also evaluated the acetylation status of α-tubulin, an essential protein for microtubule stability and neuronal survival.[28,29] α-Tubulin acetylation has been shown to regulate the integrity of the cytoskeleton, and its modification can influence neuronal function and regeneration[40]; previous publications highlighted that HDAC6 can deacetylate α-tubulin.[41] Our data concerning α-tubulin acetylation suggested a putative role of this mechanism for neuroprotection. This result was not unexpected, considering the biological activity of these drugs; however, the great variability among the experiments did not allow for obtaining statistically significant results. Nevertheless, when combined with OHP, SW-100 was able to preserve the integrity of acetylated α-tubulin, whereas SAHA did not provide the same level of protection.

This suggests that the neuroprotective effects of SW-100 may be linked to its ability to stabilize microtubules through increased α-tubulin acetylation.[14,28,42–44]

These findings are promising, as they suggest that HDAC6 inhibition, specifically with SW-100, could offer a dual benefit: enhancing the antitumor efficacy of OHP in CRC, while simultaneously protecting against OHP-induced neurotoxicity. The increased α-tubulin acetylation observed with SW-100 suggests that this compound could be a promising candidate for reducing peripheral neuropathy while maintaining the effectiveness of chemotherapy. These promising results obtained in in vitro models are valuable for further evaluation in more complex models, starting from the evaluation of the combination effects in in vivo models.

5. Conclusions

OHP-induced neurotoxicity is still a critical side effect that affects patients. Our findings highlight the potential of combining HDACis with chemotherapeutic agents to enhance both antitumor efficacy and minimize side effects like neurotoxicity. In addition, our results evidence that SW-100 could be a novel therapeutic strategy to alleviate OHP-induced neurotoxicity, thus potentially improving the clinical management of chemotherapy in patients undergoing OHP treatment.

Abbreviations

ATCC, American Type Culture Collection; CBS, calf bovine serum; CIPN, chemotherapy-induced peripheral neuropathy; CRC, colorectal cancer; DRG, dorsal root ganglia; HDAC, histone deacetylase; HDACi, histone deacetylase inhibitor; OHP, oxaliplatin; ROMI, romidepsin; SRB, sulphorodamine-B.

Financial support

This research was supported by the Associazione Italiana per la Ricerca sul Cancro (AIRC) [grant number: IG 2021 ID 25788].

Conflict of interest

The authors declare no conflicts of interest.

Data availability

Data will be made available on request.

CRediT authorship contribution statement

Angelica Squarzoni: Data curation, Formal analysis, Investigation, Writing – original draft. **Arianna Scuteri**: Conceptualization, Data curation, Investigation, Supervision, Writing – review and editing. **Elisabetta Donzelli**: Data curation, Formal analysis, Investigation, Supervision, Writing – review and editing. **Virginia Rodriguez-Menendez**: Data curation, Formal analysis, Investigation, Supervision, Writing – review and editing. **Guido Cavaletti**: Conceptualization, Funding acquisition, Supervision, Writing – review and editing.

Supplemental material

This article has supplemental material available at molpharm.aspetjournals.org.

References

1. Shukla S, Tekwani BL. Histone deacetylases inhibitors in neurodegenerative diseases, neuroprotection and neuronal differentiation. *Front Pharmacol*. 2020;11:537. https://doi.org/10.3389/fphar.2020.00537

2. Dokmanovic M, Clarke C, Marks PA. Histone deacetylase inhibitors: overview and perspectives. *Mol Cancer Res*. 2007;5(10):981–989. https://doi.org/10.1158/1541-7786.MCR-07-0324
3. Richon VM. Cancer biology: mechanism of antitumour action of vorinostat (suberoylanilide hydroxamic acid), a novel histone deacetylase inhibitor. *Br J Cancer*. 2006;95(suppl 1):S2–S6. https://doi.org/10.1038/sj.bjc.6603463
4. Lakshmaiah KC, Jacob LA, Aparna S, Lokanatha D, Saldanha SC. Epigenetic therapy of cancer with histone deacetylase inhibitors. *J Cancer Res Ther*. 2014;10(3):469–478. https://doi.org/10.4103/0973-1482.137937
5. Aldana-Masangkay GI, Sakamoto KM. The role of HDAC6 in cancer. *J Biomed Biotechnol*. 2011;2011:875824. https://doi.org/10.1155/2011/875824
6. Pulya S, Amin SA, Adhikari N, Biswas S, Jha T, Ghosh B. HDAC6 as privileged target in drug discovery: a perspective. *Pharmacol Res*. 2021;163:105274. https://doi.org/10.1016/j.phrs.2020.105274
7. Gomez-Sanchez JA, Patel N, Martirena F, Fazal SV, Mutschler C, Cabedo H. Emerging role of HDACs in regeneration and ageing in the peripheral nervous system: repair Schwann cells as pivotal targets. *Int J Mol Sci*. 2022;23(6):2996. https://doi.org/10.3390/ijms23062996
8. Simões-Pires C, Zwick V, Nurisso A, Schenker E, Carrupt PA, Cuendet M. HDAC6 as a target for neurodegenerative diseases: what makes it different from the other HDACs? *Mol Neurodegener*. 2013;8(1):7. https://doi.org/10.1186/1750-1326-8-7
9. Zheng YC, Kang HQ, Wang B, et al. Curriculum vitae of HDAC6 in solid tumors. *Int J Biol Macromol*. 2023;230:123219. https://doi.org/10.1016/j.ijbiomac.2023.123219
10. LoPresti P. HDAC6 in Diseases of cognition and of neurons. *Cells*. 2020;10(1):12. https://doi.org/10.3390/cells10010012
11. Kozikowski AP, Shen S, Pardo M, et al. Brain penetrable histone deacetylase 6 inhibitor SW-100 ameliorates memory and learning impairments in a mouse model of fragile X syndrome. *ACS Chem Neurosci*. 2019;10(3):1679–1695. https://doi.org/10.1021/acschemneuro.8b00600
12. Karagiannis D, Rampias T. HDAC inhibitors: dissecting mechanisms of action to counter tumor heterogeneity. *Cancers (Basel)*. 2021;13(14):3575. https://doi.org/10.3390/cancers13143575
13. Shi TJ, Huang P, Mulder J, Ceccatelli S, Hokfelt T. Expression of p-Akt in sensory neurons and spinal cord after peripheral nerve injury. *Neurosignals*. 2009;17(3):203–212. https://doi.org/10.1159/000210400
14. Zhang Y, Li N, Caron C, et al. HDAC-6 interacts with and deacetylates tubulin and microtubules in vivo. *EMBO J*. 2003;22(5):1168–1179. https://doi.org/10.1093/emboj/cdg115
15. Cavaletti G. Chemotherapy-induced peripheral neurotoxicity (CIPN): what we need and what we know. *J Peripher Nerv Syst*. 2014;19(2):66–76. https://doi.org/10.1111/jns5.12073
16. Arango D, Wilson AJ, Shi Q, et al. Molecular mechanisms of action and prediction of response to oxaliplatin in colorectal cancer cells. *Br J Cancer*. 2004;91(11):1931–1946. https://doi.org/10.1038/sj.bjc.6602215
17. Misset JL, Bleiberg H, Sutherland W, Bekradda M, Cvitkovic E. Oxaliplatin clinical activity: a review. *Crit Rev Oncol Hematol*. 2000;35(2):75–93. https://doi.org/10.1016/S1040-8428(00)00070-6
18. Kuipers EJ, Grady WM, Lieberman D, et al. Colorectal cancer. *Nat Rev Dis Primers*. 2015;1(1):15065. https://doi.org/10.1038/nrdp.2015.65
19. Zajączkowska R, Kocot-Kępska M, Leppert W, Wrzosek A, Mika J, Wordliczek J. Mechanisms of chemotherapy-induced peripheral neuropathy. *Int J Mol Sci*. 2019;20(6):1451. https://doi.org/10.3390/ijms20061451
20. Staff NP, Cavaletti G, Islam B, Lustberg M, Psimaras D, Tamburin S. Platinum-induced peripheral neurotoxicity: from pathogenesis to treatment. *J Peripher Nerv Syst*. 2019;24(S2):S26–S39. https://doi.org/10.1111/jns.12335
21. Martínez-Maqueda D, Miralles B, Recio I. HT29 cell line. In: Verhoeckx K, Cotter P, López-Expósito I, eds. *The Impact of Food Bioactives on Health*. Springer; 2015:113–124. https://doi.org/10.1007/978-3-319-16104-4_11
22. Jumarie C, Malo C. Caco-2 cells cultured in serum-free medium as a model for the study of enterocytic differentiation in vitro. *J Cell Physiol*. 1991;149(1):24–33. https://doi.org/10.1002/jcp.1041490105
23. Chen TR, Dorotinsky CS, McGuire LJ, Macy ML, Hay RJ. DLD-1 and HCT-15 cell lines derived separately from colorectal carcinomas have totally different chromosome changes but the same genetic origin. *Cancer Genet Cytogenet*. 1995;81(2):103–108. https://doi.org/10.1016/0165-4608(94)00225-z
24. Marchetti P, Galla DA, Russo FP, et al. Apoptosis induced by oxaliplatin in human colon cancer HCT15 cell line. *Anticancer Res*. 2004;24(1):219–226.
25. Scuteri A, Cassetti A, Tredici G. Adult mesenchymal stem cells rescue dorsal root ganglia neurons from dying. *Brain Res*. 2006;1116(1):75–81. https://doi.org/10.1016/j.brainres.2006.07.127
26. Motulsky HJ, Head T, Clarke PBS. Analyzing lognormal data: a nonmathematical practical guide. *Pharmacol Rev*. 2025;77(3):100049. https://doi.org/10.1016/j.pharmr.2025.100049
27. Brentnall M, Rodriguez-Menocal L, De Guevara RL, Cepero E, Boise LH. Caspase-9, caspase-3 and caspase-7 have distinct roles during intrinsic apoptosis. *BMC Cell Biol*. 2013;14(1):32. https://doi.org/10.1186/1471-2121-14-32
28. Maruta H, Greer K, Rosenbaum JL. The acetylation of alpha-tubulin and its relationship to the assembly and disassembly of microtubules. *J Cell Biol*. 1986;103(2):571–579. https://doi.org/10.1083/jcb.103.2.571
29. Li L, Yang XJ. Tubulin acetylation: responsible enzymes, biological functions and human diseases. *Cell Mol Life Sci*. 2015;72(22):4237–4255. https://doi.org/10.1007/s00018-015-2000-5
30. Hwang JY, Aromolaran KA, Zukin RS. The emerging field of epigenetics in neurodegeneration and neuroprotection. *Nat Rev Neurosci*. 2017;18(6):347–361. https://doi.org/10.1038/nrn.2017.46
31. Cavaletti G, Marmiroli P. Management of oxaliplatin-induced peripheral sensory neuropathy. *Cancers (Basel)*. 2020;12(6):1370. https://doi.org/10.3390/cancers12061370
32. Chen X, Gan Y, Au NPB, Ma CHE. Current understanding of the molecular mechanisms of chemotherapy-induced peripheral neuropathy. *Front Mol Neurosci*. 2024;17:1345811. https://doi.org/10.3389/fnmol.2024.1345811
33. Zhang J, Ma J, Trinh RT, Heijnen CJ, Kavelaars A. An HDAC6 inhibitor reverses chemotherapy-induced mechanical hypersensitivity via an IL-10 and macrophage dependent pathway. *Brain Behav Immun*. 2022;100:287–296. https://doi.org/10.1016/j.bbi.2021.12.005
34. Ma J, Trinh RT, Mahant ID, et al. Cell-specific role of histone deacetylase 6 in chemotherapy-induced mechanical allodynia and loss of intraepidermal nerve fibers. *Pain*. 2019;160(12):2877–2890. https://doi.org/10.1097/j.pain.0000000000001667
35. Cavaletti G, Canta A, Chiorazzi A, et al. ITF6475, a new histone deacetylase 6 inhibitor, prevents painful neuropathy induced by paclitaxel. *Toxics*. 2025;13(9):767. https://doi.org/10.3390/toxics13090767
36. Cheng Y, He C, Wang M, et al. Targeting epigenetic regulators for cancer therapy: mechanisms and advances in clinical trials. *Signal Transduct Target Ther*. 2019;4(1):62. https://doi.org/10.1038/s41392-019-0095-0
37. Watson AJ. Apoptosis and colorectal cancer. *Gut*. 2004;53(11):1701–1709. https://doi.org/10.1136/gut.2004.052704
38. Calls A, Carozzi V, Navarro X, Monza L, Bruna J. Pathogenesis of platinum-induced peripheral neurotoxicity: insights from preclinical studies. *Exp Neurol*. 2020;325:113141. https://doi.org/10.1016/j.expneurol.2019.113141
39. Joseph EK, Levine JD. Caspase signalling in neuropathic and inflammatory pain in the rat. *Eur J Neurosci*. 2004;20(11):2896–2902. https://doi.org/10.1111/j.1460-9568.2004.03750.x
40. Black MM, Baas PW, Humphries S. Dynamics of α-tubulin deacetylation in intact neurons. *J Neurosci*. 1989;9(1):358–368. https://doi.org/10.1523/jneurosci.09-01-00358.1989
41. English K, Barton MC. HDAC6: A key link between mitochondria and development of peripheral neuropathy. *Front Mol Neurosci*. 2021;14:684714. https://doi.org/10.3389/fnmol.2021.684714
42. Bahram Sangani N, Koetsier J, Mélius J, et al. A novel insight into neurological disorders through HDAC6 protein–protein interactions. *Sci Rep*. 2024;14(1):14666. https://doi.org/10.1038/s41598-024-65094-1
43. Chen S, Owens GC, Makarenkova H, Edelman DB. HDAC6 regulates mitochondrial transport in hippocampal neurons. *PLoS One*. 2010;5(5):e10848. https://doi.org/10.1371/journal.pone.0010848
44. Adalbert R, Kaieda A, Antoniou C, et al. Novel HDAC6 inhibitors increase tubulin acetylation and rescue axonal transport of mitochondria in a model of Charcot–Marie–Tooth type 2F. *ACS Chem Neurosci*. 2020;11(3):258–267. https://doi.org/10.1021/acschemneuro.9b00338